a

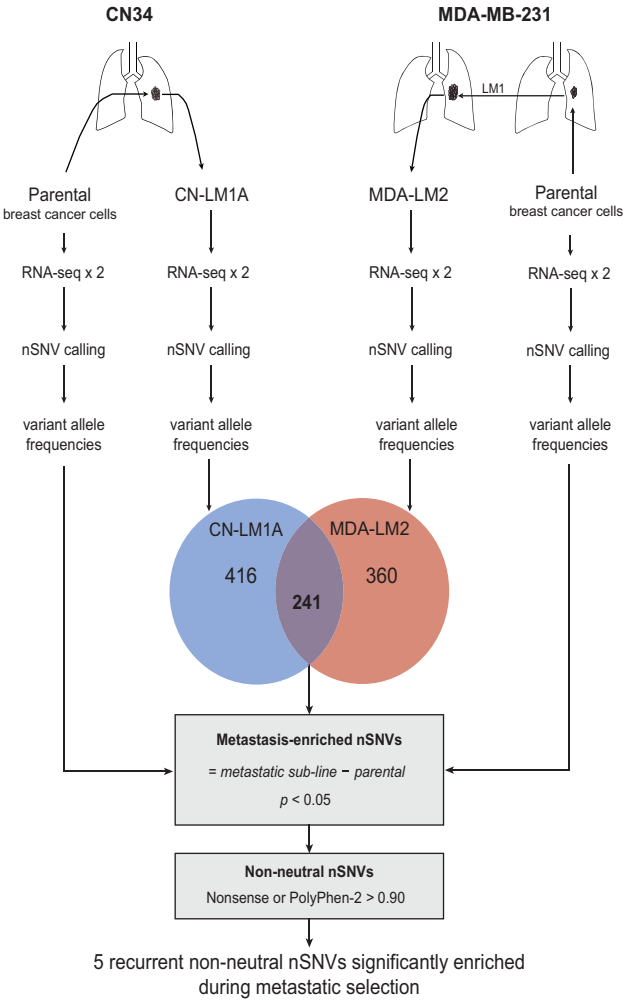

b

nSNVs recurrently enriched during breast cancer metastasis

Gene	Genomic location	Base	Amino acid	fold-enrichment CN-LM1A	fold-enrichment MDA-LM2	*p*-value	Protein function	Mutated domain	PolyPhen 2 HumDiv
PANX1	11:93526390	**C268T**	**Q90***	**1.53** **1.46**	**1.48** **1.20**	**0.0023**	Plasma membrane megachannel	ECL1	**Nonsense**
RBFA	18:75906883	**G773T**	**G258V**	**1.70** **1.35**	**1.16** **1.44**	**0.0112**	Mitochondrial ribosome binding factor	GatB	**1.00**
REST	4:57492601	**G2821C**	**D941H**	**1.08** **1.28**	**1.23** **1.09**	**0.0372**	RE1-silencing transcription factor	C-terminal	**0.987**
KRIT1	7:91668596	**G1958A**	**S701N**	**1.47** **2.12**	**1.18** **1.28**	**0.0473**	Positive regulator of integrin-β1 signaling	Rap1a binding	**0.963**
ZSWIM6	5:60861703	**G1906A**	**V636M**	**1.22** **1.23**	**1.04** **1.19**	**0.0295**	Zinc finger SWIM-type 6	-	**0.906**

c

Allele-specific RNA-seq (biological triplicates)	**CN-LM1A**	**MDA-LM2**
Mean enrichment (%)	5.44	5.74
***P*-value**	0.02	0.01

d

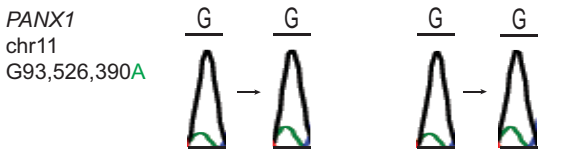

e

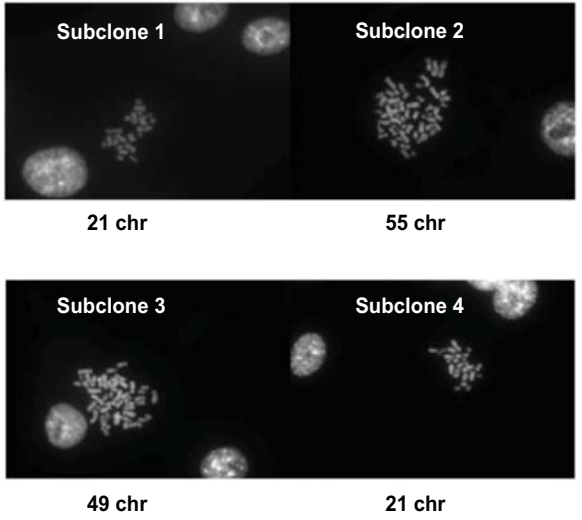

Supplementary Figure 1

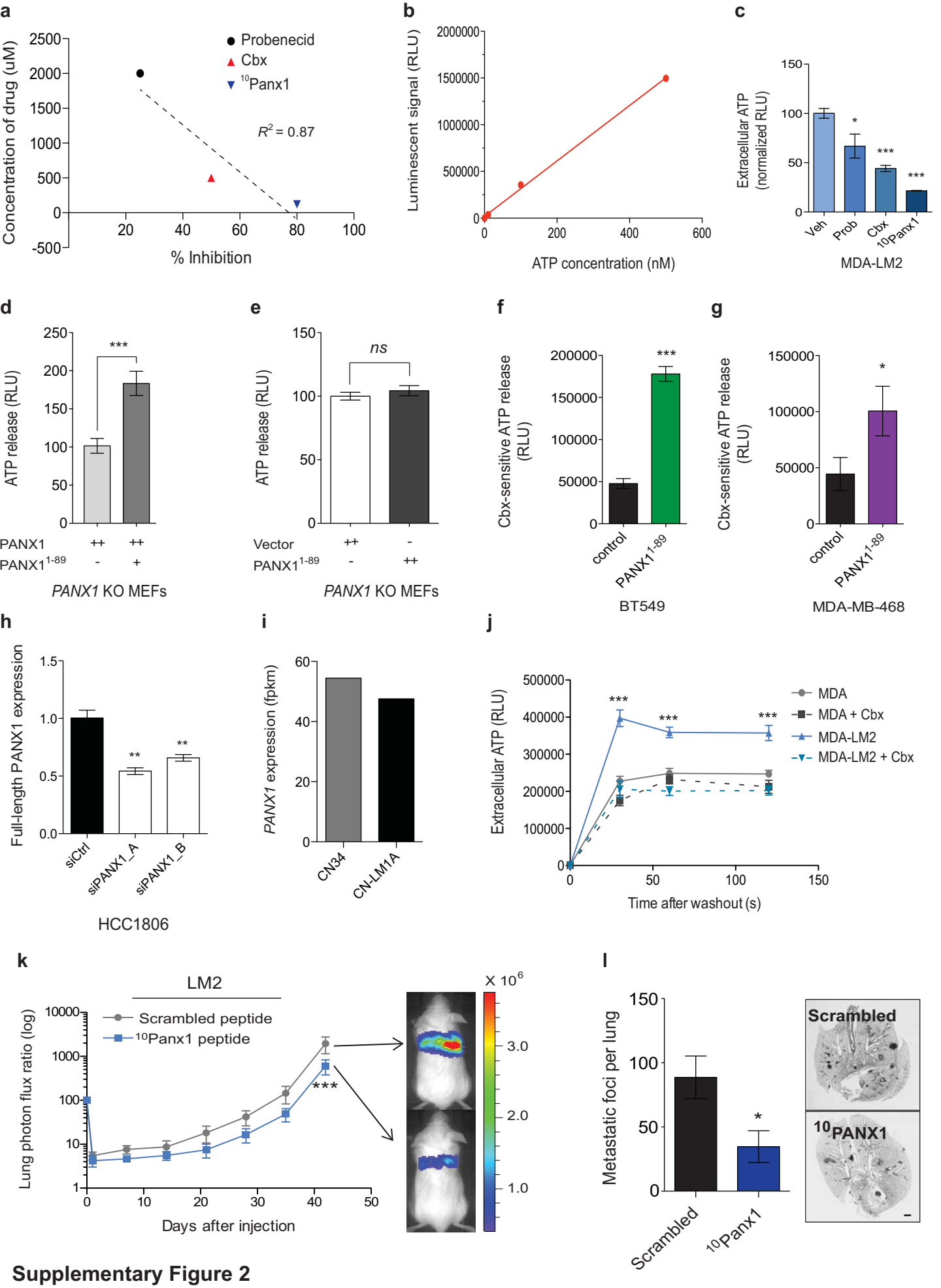

Supplementary Figure 2

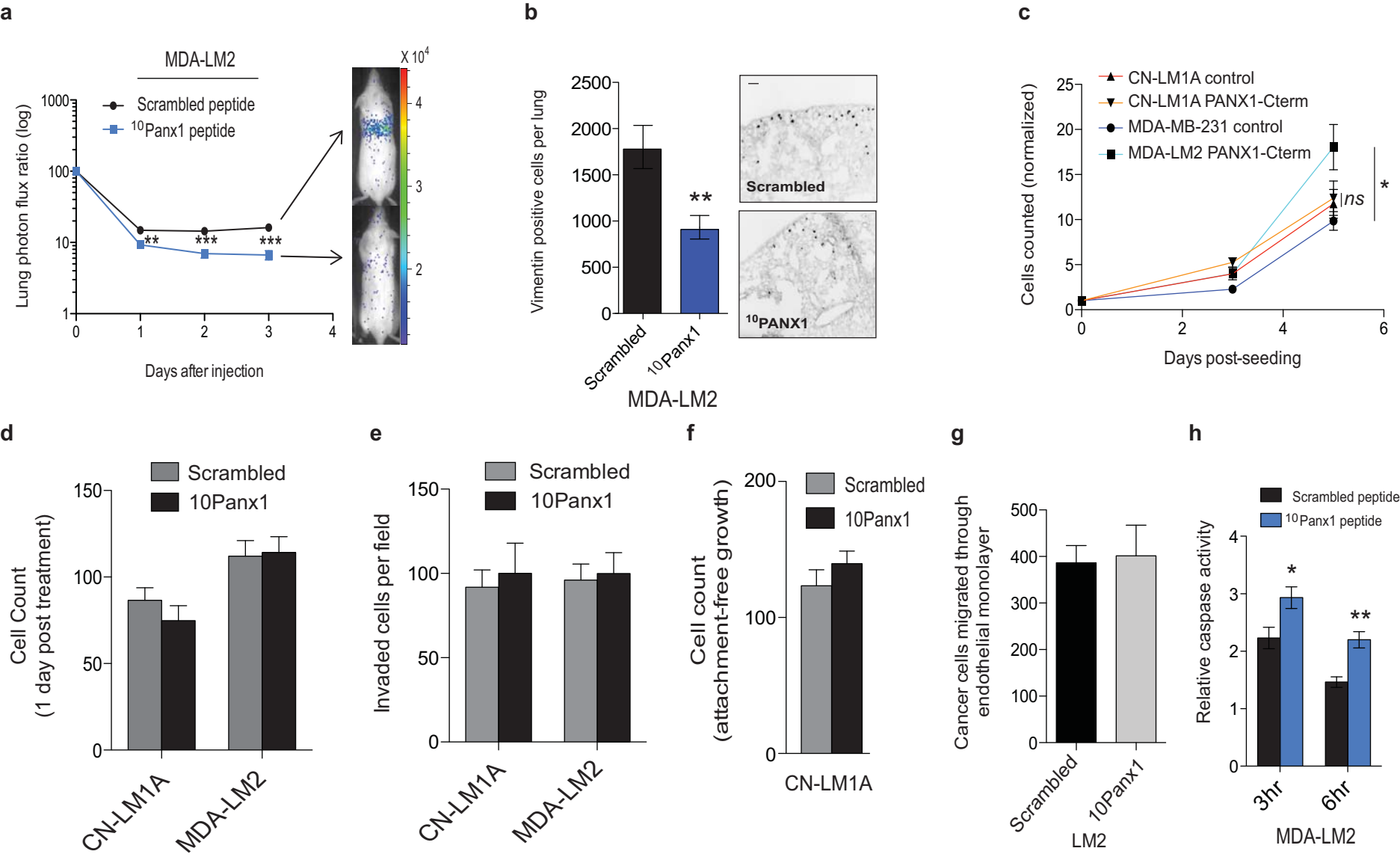

Supplementary Figure 3

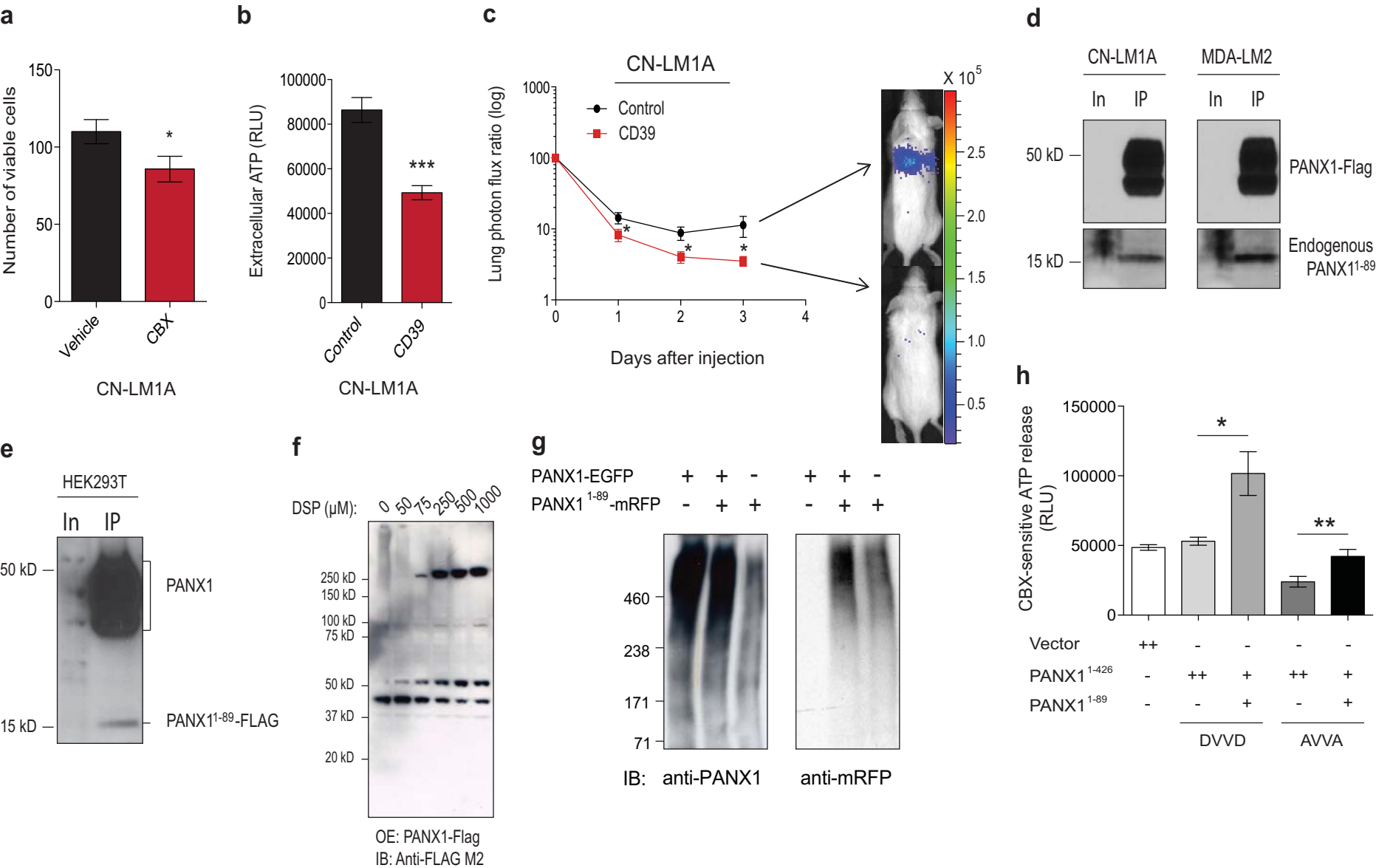

Supplementary Figure 4

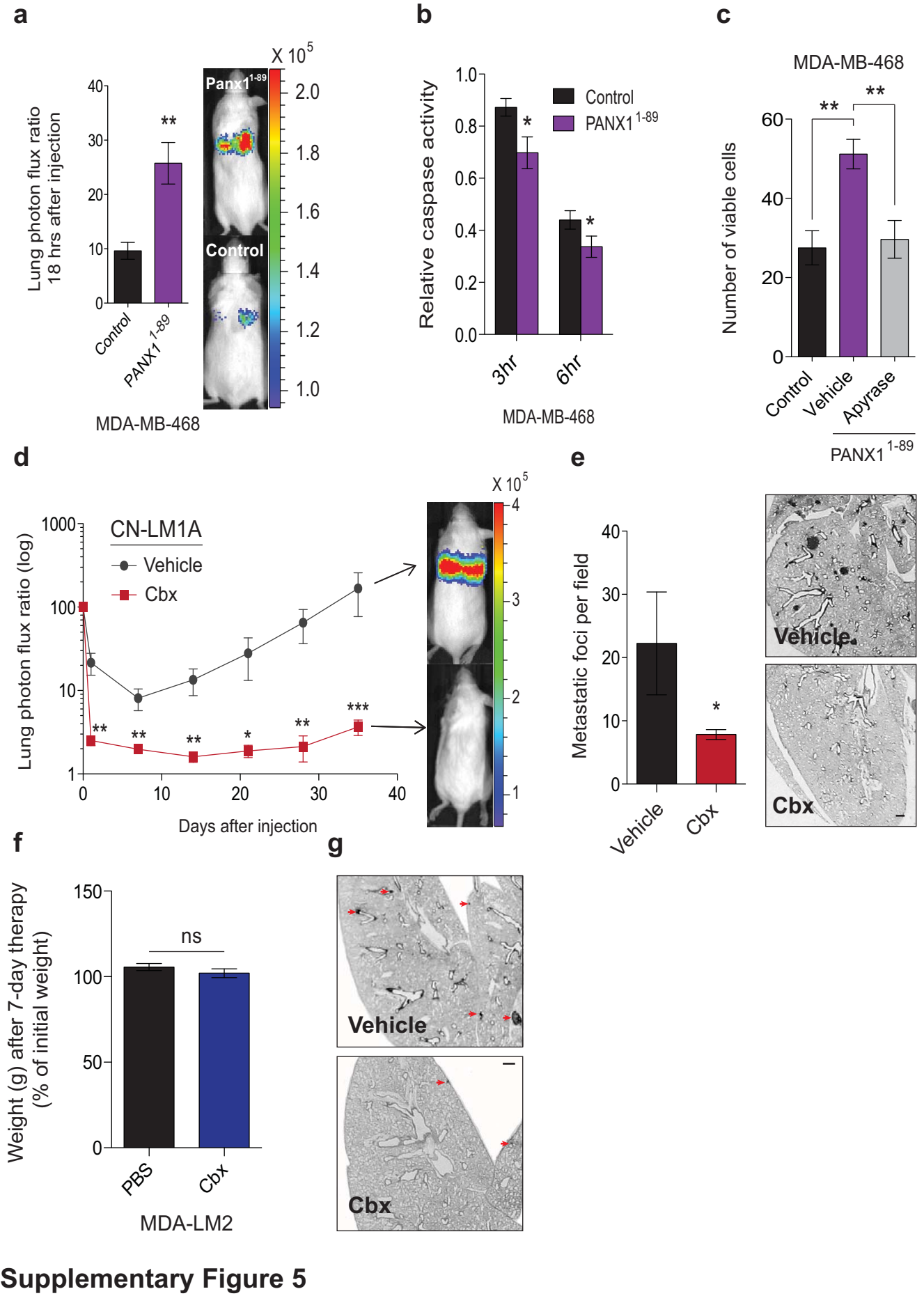

Supplementary Figure 5

Supplementary Figure 1. The discovery of recurrent mutations enriched in highly metastatic breast cancer. a, Schematic of the systematic discovery framework used to identify nSNVs enriched by allelic frequency in highly metastatic CN-LM1A and MDA-LM2 human breast cancer cells. **b**, Recurrent and non-neutral mutations identified to be significantly enriched in highly metastatic breast cancer cells by a one-tailed Student's *t*-test ($P < 0.05$); $n = 4$. **c**, Allele-specific RNA-seq of the *PANX1 C268T* allele in biological triplicates of the CN34 and MDA-MB-231 parental breast cancer cells and their respective lung metastatic derivatives, CN-LM1A and MDA-LM2. Mean enrichment was quantified by counting the increase in frequency of the *PANX1 C268T* allele in the metastatic sub-lines as compared to the corresponding parental lines; $n = 3$. **d**, Sanger sequencing of the *PANX1* mutant allele from genomic DNA of each parental and metastatic line. **e**, Metaphase spread of four single-cell subclones generated from the MDA-LM2 cell population showing the intraclonal genetic heterogeneity (varying number of chromosomes) of *in vivo* selected highly metastatic derivative cell lines. Fractional enrichment of nSNVs in metastatic derivatives can be understood in the context of such heterogeneity. *n* represents biological replicates. Experiments **b**–**d** are representative and were replicated with two independent metastatic breast cancer cell lines.

Supplementary Figure 2. PANX1$^{1-89}$ augments PANX1 channel-mediated extracellular ATP release from metastatic breast cancer cells. a, The % inhibition of extracellular ATP release from metastatic derivative sub-lines at one minute was measured in the presence of three independent PANX1 inhibitors (Probenecid, Cbx and ^{10}Panx1) at varying concentrations (2 mM, 500 μM and 100 μM, respectively). **b**, Increasing concentrations of ATP (0, 50, 100, 500 nM) were measured using the Cell-Titer Glo luciferase assay. **c**, Quantification of PANX1-mediated ATP release from the MDA-LM2 sub-line pretreated for 10 min with PBS, 2mM probenecid (Prob), 500 μM CBX, or 100 μM ^{10}Panx1 peptide; $n = 4$. **d,** Extracellular ATP release from *PANX1*-null mouse embryonic fibroblasts (*PANX1* KO MEFs) transfected with 5 μg human full-length PANX1 or 5 μg human full-length PANX1 and 2.5 μg human PANX1$^{1-89}$; $n = 7$. **e**, Extracellular ATP release from *PANX1* KO MEFs transfected with 5 μg human PANX1$^{1-89}$ or 5 μg vector control; $n = 8$. **f**, PANX1-mediated extracellular ATP release from BT549 breast cancer cells expressing PANX1$^{1-89}$ or control vector; $n = 8$. **g**, PANX1-mediated extracellular ATP release from MDA-MB-468 breast cancer cells expressing PANX1$^{1-89}$ or control vector; $n = 8$. **h**, Quantitative RT-PCR analysis of wild-type *PANX1*

transcript expression in HCC1806 cells expressing $PANX1^{1-89}$ transfected with two independent siRNAs that specifically target full-length *PANX1*; *n* = 4. **i**, CN34 and CN-LM1A total PANX1 mRNA expression quantified by RNA-seq; FPKM values averaged over two rounds (4 technical replicates) of RNA-seq for each cell line; *n* = 2. **j**, Time-course measurements of ATP release from MDA-MB-231 parental cells and the MDA-LM2 metastatic derivatives sub-lines pretreated with Cbx (500 μM) or PBS for 10 min; *n* = 4. **k**, Quantitative bioluminescence imaging of lung metastasis after the injection of 4×10^4 MDA-LM2 breast cancer cells pretreated with 100 μM ^{10}Panx1 or scrambled peptide, into NOD scid (NS) mice; *n* = 5. **l**, Day 42 quantification of metastatic foci from H&E-stained lungs (left) and representative lung images from vimentin-stained lungs (right) of mice injected with MDA-LM2 cells pretreated with ^{10}Panx1 or scrambled peptide; *n* = 5. Scale bar, 1 mm. Error bars, s.e.m., *ns*, nonsignificant, *, $P < 0.05$; **, $P < 0.01$; ***, $P < 0.001$ by a one-tailed Student's *t*-test. *n* represents biological replicates. Experiments **c**–**g** and **i–l** were replicated twice with two independent cell lines. Experiments **h** and **i** are single experiments with biological replicates. Bioluminescent and histological images are representative of the median.

Supplementary Figure 3. PANX1 activity promotes the metastatic dissemination of breast cancer cells by enhancing early survival in the target organ. a, Daily quantitative imaging plot of lung bioluminescence subsequent to the injection of 4×10^4 metastatic MDA-LM2 breast cancer cells pretreated (30 min) with 100 μM ^{10}Panx1 or scrambled peptides, into NS mice; *n* = 7. **b**, Lungs from mice were extracted at day 3, sectioned and stained for vimentin and the numbers of vimentin-positive cancer cells were quantified; *n* = 7. Scale bar, 0.25 mm. **c**, Quantification of proliferation over 5 days for CN-LM1A and MDA-LM2 cells over-expressing the autoinhibitory C-terminal domain of PANX1 or control vector; *n* = 4. **d**, Quantification of 24 hour cell survival for CN-LM1A and MDA-LM2 cells pretreated for 15 min with 100μM ^{10}Panx1 or scrambled peptide; *n* = 8. **e**, Quantification of 24 hour invasion for CN-LM1A and MDA-LM2 cells in the presence of 100μM ^{10}Panx1 or scrambled peptide; *n* = 4. **f**, Quantification of 36 hour anchorage-independent cancer cell survival for CN-LM1A cells in the presence of 100 μM ^{10}Panx1 or scrambled peptide; *n* = 4. **g**, Quantification of 24 hour trans-endothelial migration for MDA-LM2 cells in the presence of 100 μM ^{10}Panx1 or scrambled peptide; *n* = 4. **h**, *In vivo* quantification of luciferase-based caspase-3/7 activity at 3 and 6 hrs after tail-vein injection of 4×10^4 MDA-LM2 breast cancer cells, pretreated with 100 μM

^{10}Panx1 or scrambled peptide, into NS mice; n = 5. Error bars, s.e.m., *, $P < 0.05$; **, $P < 0.01$; ***, $P < 0.001$ by a one-tailed Student's t-test. n represents biological replicates. Experiments **a**–**e** and **h** were replicated with at least two times in two independent cell lines. Experiments **f** and **g** are single experiments with biological replicates. Bioluminescent and histological images are representative of the median.

Supplementary Figure 4. PANX1$^{1-89}$ augments ATP release through an interaction with PANX1 to promote breast cancer cell survival in the pulmonary vasculature. **a**, Quantification of viable, trypan blue-negative CN-LM1A cells with 30 min Boyden chamber centrifugation (3,800 rpm) after cells were pre-treated for 10 min with 500 μM CBX or PBS; n = 4. **b**, Quantification of extracellular ATP release from CN-LM1A cells expressing the extracellular ATP hydrolase CD39 or control vector; n = 8. **c**, Daily quantitative imaging of lung bioluminescence for three days subsequent to the injection of 1 × 10^5 CN-LM1A breast cancer cells expressing CD39 or control vector, into NS mice; n = 6. **d**, Co-immunoprecipiation of Flag-tagged full-length PANX1$^{1-426}$ and endogenous PANX1$^{1-89}$ from CN-LM1A and MDA-LM2 cells. Anti-PANX1 N-terminal antibody detected a band similar in size to that of Flag-tagged PANX1$^{1-89}$ expressed in HEK293T cells. The presence of this band in the metastatic sub-lines suggests that endogenous PANX1$^{1-89}$ associates with Flag-tagged full-length PANX1$^{1-426}$. The multiple bands representing full-length PANX1 represent the previously described glycosylated forms of PANX1. **e**, Co-immunoprecipitation of PANX1$^{1-89}$-Flag from HEK293T cells co-transfected with full-length PANX1$^{1-426}$. Anti-PANX1 N-terminal antibody was used to detect the associated PANX1 species. The multiple full-length PANX1 bands represent the previously described glycosylated forms of PANX1. The input lysates were immunoblotted for PANX1. **f**, Increasing concentrations of DSP (dithiobis[succinimidyl propionate]) crosslinker were applied to HEK293T cells expressing Flag-tagged PANX1 prior to lysis. PANX1 complexes were detected using anti-FLAG M2 antibody. **g**, Anti-PANX1 and anti-RFP immunoblotting of DSP crosslinked lysates from HEK293T cells expressing PANX1-EGFP, PANX1-EGFP and PANX1$^{1-89}$-mRFP or PANX1$^{1-89}$-mRFP. Molecular weights are indicated. **h**, Quantification of PANX1-mediated ATP release from HEK293T cells transfected with 5 μg control vector, 5 μg wild-type PANX1 (DVVD), 2.5 μg wild-type PANX1 and 2.5 μg PANX1$^{1-89}$, 5 μg caspase resistant full-length PANX1 (AVVA), or 2.5 μg caspase resistant full-length PANX1 and 2.5 μg PANX1$^{1-89}$; n = 4.

Error bars, s.e.m., *, $P < 0.05$; **, $P < 0.01$; ***, $P < 0.001$ by a one-tailed Student's *t*-test. *n* represents biological replicates. Experiments **a**–**d** were replicated at least two times with at least two independent cell lines. Experiments **e**–**h** are single experiments with biological replicates. Bioluminescent and images are representative of the median.

Supplementary Figure 5. PANX1 is a druggable target promoting breast cancer metastasis upon cancer cell entry into the lung. a, Quantitative imaging of lung bioluminescence 18 hrs post tail-vein injection of 1×10^6 MDA-MB-468 breast cancer cells, expressing $PANX1^{1-89}$ or a control vector, into NSG mice; *n* = 6. **b**, *In vivo* quantification of luciferase-based caspase-3/7 activity at 3 and 6 hrs post tail-vein injection of 1×10^6 MDA-MB-468 breast cancer cells, expressing either $PANX1^{1-89}$ or a control vector, into NS mice; *n* = 6. **c**, Quantification of viable, trypan blue-negative MDA-MDA-468 cells expressing $PANX1^{1-89}$ or a control vector after 1 hr extreme hypotonic (12.5% PBS) stretch in the presence of succinate buffer or apyrase (2U/ml); *n* = 4. **d**, Quantitative bioluminescence imaging of lung metastasis after tail-vein injection of 1×10^5 CN-LM1A breast cancer cells pretreated for 30 min with CBX (500 μM) or PBS vehicle into NS mice; *n* = 4 (vehicle), *n* = 6 (Cbx). **e**, Day 35 quantification of metastatic foci (left) and representative lung images (right) from H&E stained lungs of mice injected with CN-LM1A cells pretreated with CBX or PBS vehicle; *n* = 4 (vehicle), *n* = 6 (Cbx). Scale bar, 0.5 mm. **f**, Mouse body weight before and after daily i.p. injections of CBX (25 mg/kg) or an equivalent volume of PBS vehicle for seven days. *n* = 10. **g**, 4-week representative images of vimentin-stained lungs from mice treated with two 25 mg/kg doses of intravenous CBX or vehicle control. Arrowheads indicate vimentin-positive metastatic foci. Scale bar, 0.5 mm. Error bars, s.e.m., *ns*, nonsignificant; *, $P < 0.05$; **, $P < 0.01$; ***, $P < 0.001$ by a one-tailed Student's *t*-test. *n* represents biological replicates. Experiments **a**–**c** were replicated at least two times with at least two independent cell lines. Therapeutic PANX1 inhibition experiments were performed using differing protocols with two independent triple negative breast cancer cell lines. Bioluminescent and histological images are representative of the median.

Supplementary Table 1. RNA-seq profile of CN34, CN-LM1A, MDA-MB-231 and MDA-LM2 cell populations.

Supplementary Table 2. Primers used in this study.